Journal of Data Acquisition and Processing
ISSN: 1004-9037
https://sjcjycl.cn/
DOI: 10.5281/zenodo.98549928

SURFACE CONDUCTIVITY EFFECT ON EVAPORATION OF DROPLET

Rupak Kumar Deb[a] Sanjay Sundriyal [b]

Iqbal Ahmed Khan [c a b] Lingaya's Vidyapeeth, Faridabad, Haryana, [c]Greater Noida Institute of Technology, Greater Noida, Uttar Pradesh

ABSTRACT

Evaporation of droplet is a strong requirement of many devices as the fogging is a critical problem for operation for such devices. Many devices are using transparent heaters. At the same time the deposition of droplet on working surfaces or exposed surfaces for long time is also not allowed for certain cases. These problem leads to study the behavior of droplet and its evaporation on exposed surfaces. Many experiments has been done during past 3 decades on the dependence and influence of various parameters over the evaporation of droplet. For the combination of unwetted substrate surface, the liquid droplet and the water vapor buoyancy of the atmosphere, there is quantitative agreement of Newton's law of cooling. In this paper we do the mathematical modeling of droplet evaporation with the substrate temperature.

KEYWORDS: DROPLET; DEFOGGING; DEFROSTING; EVAPORATION; HYDROPHOBIC; THERMAL CONDUCTIVITY; MARANGONI EFFECT; TRANSPARENT HEATERS; SESSILE

1. INTRODUCTION

With the growing interest of scientific and important technological problems of liquid droplet evaporation, more study is initiated focusing the behavior of evaporation of a droplet in recent past. The evaporation of a droplet on the basis of constant angle of contact and on the basis of constant area of contact has been studied by Picknett and Bexon (1) in the year 1977 and suggested a theoretical model assuming that the surface just above the droplet contains saturated vapor and the liquid vapour that diffuses from the liquid droplet is the process which is rate –limiting type ((2) and (3)). (1) found the solution for net mass flux diffusion from droplet surface by using the solution of electrical potential for a lens shaped charged conductor ((4)). At the same time Bourge's- Monnier and Shanahan (5) also labeled four sharp stages for the process of evaporation and also found the solution for net mass flux diffusion from droplet surface. Interestingly during the process of evaporation and subsequent drying up of the droplet, the dispersed solids within the droplet produces a ring strain at the contact lines . This phenomena was theoretically modeled by Deegan et al.((6), (7)). The contact angle of the droplet with respect to the substrate is a function of mass flux of evaporation of a droplet. Hu and Larson (8) used finite element method

CONTACT Rupak Kumar Deb. Email: deb.rupak@gmail.com

Substrate	$\kappa s(Kgms{-}3K{-}1)$	$\rho_l(Kgm^{-3})$	$cp(m2s{-}2K{-}1)$
Al	237	2.71×10^3	913
MS	37.5	7.8×10^3	510.7

Table 1. The numerical test domain parameters and vehicle speed and acceleration parameters.

and obtained an approximation about the fact of the relationship between the mass flux and the contact angle and later Hu and Larson ((9)) further suggested the thermocapillary effect known as Maragnoni effect by generalizing the numerical analysis of the flow inside the droplet Hu and Larson ((10)). Ristenpart et al. (11) studied recirculation due to thermocapillary action and observed that the relative thermal conductivity of the substrate and the droplet fluid along with the contact angle governs the recirculation within the droplet. All the work described above are theoretical assuming that layer above the free surface of the droplet is saturated with vapor .The evaporation of a droplet in hot environment and the formation of hot wave from center of the evaporating droplet towards the boundary was studied by Koffi Sagna et al.(2013) .The evaporation character of suspended droplet was measured by WANG et al.(12). A new mathematical model developed by analyzing mathematically on the basis of energy balance , steady state mass flux and momentum equation for a evaporating droplet surrounded by air and vapor mixture environment was given recently by Tonini et al.(13). Charitatos et al.(14) developed a model to study the effect of the inclination of substrate over the evaporation effect of droplet and concluded that the steeper substrate decreases the rate of evaporation of droplet. Raju et al.(15) suggested that during evaporation of a binary droplet, the accumulation of the particles occurs at a particular radius where there is interface between liquid and air along with the accumulation along the substrate contact line. This accumulation at a particular radius produces a ring known as Marangoni ring. Most of above discussed experiment of evaporation of droplet has used various substrates , liquids , substrate angles , contact angles but without considering the effect of thermal conductivity of different substrates. In this paper we will include saturation concentration variation with temperature and couple with atmospheric humidity to reproduce and justify the experimental outcome with the help of a basic model.

2. EXPERIMENTAL PROCEDURE

The figure 1 illustrates the experimental set-up. The process of experiment involves the observation of the behavior during the evaporation of a droplet deposited over a two different substrates having different thermal conductivity. The droplet of pure liquid is being deposited over the different substrates with a fixed volume dispersible apparatus. The substrates taken are Aluminum (Al) and Mild Steel (MS) having different values of thermal conductivity and both the specimen have dimension 1.2cm X 1.2 cm X 0.1 cm (length x width X thickness). The droplet used is water and the Contact angles observed was 57^0 for water. The table **??** provides the physical properties of substrates on which droplet evaporates. The experiments were performed at an atmospheric pressure of 99.2KPa whereas the ambient temperatures as well as relative humidity were varied inside the enclosure by lighting the bulb of different power of $100W$.$200W$ and $260W$. The droplets were formed using a controlled device and all the droplets were found to be having spherical cap. The base temperature was varied using a controlled heater and the time of evaporation were noted. The table 1

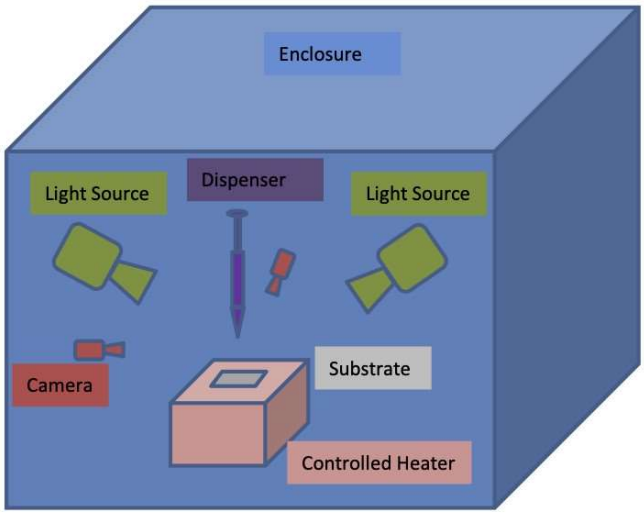

Figure 1. Experimental set-up is depicted in this figure

provides the physical properties of substrates on which droplet evaporates.

3. NUMERICAL ALGORITHM

Governing Equations

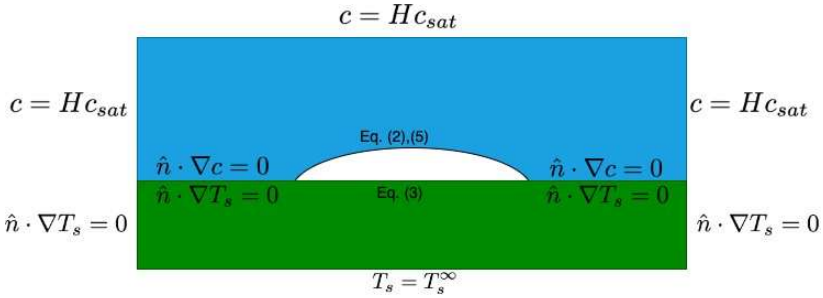

Figure 2. The boundary condition for droplet heat transport, solid body heat transport and vapor mass transport equation is depicted in the figure.

The figure 2 illustrates the droplet region, vapor region (blue) and solid body region (green) with the corresponding boundary conditions. Assuming a steady state condition, the governing heat transport equation in the droplet surface is given as

$$\nabla^2 T_d = 0, \tag{1}$$

where ∇ corresponds to gradient operator and T_d represents the droplet temperature.

The droplet loses heat via evaporation on the droplet surface and it gains heat via heat transport through substrate interface. On the droplet surface, the heat flux can be related with evaporation massflux as

$$Q = -\kappa_d(\hat{n} \cdot \nabla T_d) = \mathrm{L}(\hat{n} \cdot D\nabla c), \tag{2}$$

where Q represents heat flux, $\hat{n}$ corresponds to unit normal vector to the droplet surface, L represents latent heat of vaporization and c corresponds to the vapor concentration at the droplet-air interface. The term κ_d represents the thermal conductivity for the droplet fluid and D represents the diffusion coefficient of the vapor. The boundary condition at the substrate-droplet interface corresponds to the continuity of heat flux at the solid-droplet interface. This corresponds to

$$\kappa_d \frac{\partial T_d}{\partial y} = \kappa_s \frac{\partial T_s}{\partial y}, \tag{3}$$

where the terms κ_s represents the thermal conductivity of the solid, T_s represents the solid body temperature and y corresponds to the vertical coordinate at the droplet-solid interface.

Mass flux of due to evaporation at the droplet surface leads to enhanced concentration near the droplet, which diffuses into the saturated vapor concentration at large distance from the droplet. Using steady state and negligible convective flux assumption for the vapor phase, the governing mass transport equation for the vapor phase in the neighboring region of droplet is given as

$$\nabla^2 c = 0. \tag{4}$$

A the droplet interface, the assumption of saturated vapor concentration is used for vapor phase as described by Dunn et. al. (16), which leads to

$$c_{sat}(T) = c_{sat}(T_a) + \frac{\partial c_{sat}}{\partial T}\Big|_{T=T_a}(T - T_a), \tag{5}$$

where T_a corresponds to ambient air temperature and c_{sat} represents the saturated vapor concentration. The unwetted surface corresponds to no mass flux for the vapor. Therefore, on the unwetted solid surface near the droplet, the neumann boundary condition is used for the vapor concentration i.e.

$$\frac{\partial c}{\partial y} = 0. \tag{6}$$

In the rest of the surfaces, a far field partially saturated vapor condition is used, which corresponds to

$$c = Hc_{sat}(T_a), \tag{7}$$

where H represents the humidity.

For the solid body, using the assumption of steady state condition, the heat transport equation becomes

$$\nabla^2 T_s = 0. \tag{8}$$

The far field condition used here are the Neumann condition along vertical surface and unwetted interface with air for the solid. At a depth from in the solid surface, a Dirichlet condition is applied which corresponds to the solid body temperature. The continuity of temperature condition is applied at the droplet.solid interface.

Numerical Algorithm

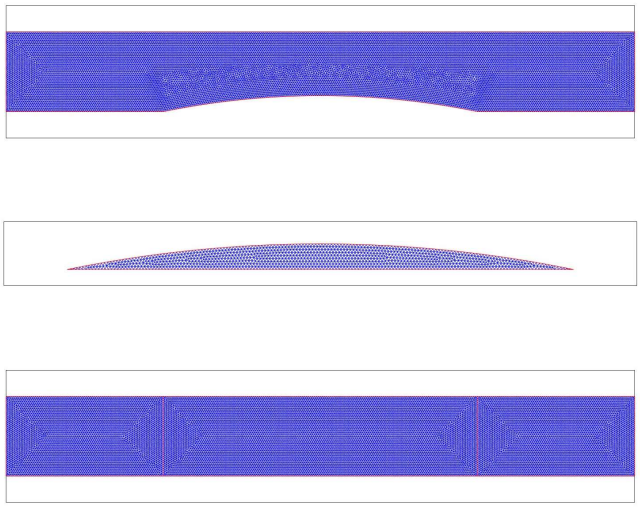

Figure 3. Meshing of droplet (center), vapor region (top) and solid region (bottom) are illustrated here.

The following set of steps describe the numerical algorithm to solve this coupled mass and heat transfer equations for droplet, surrounding air and substrate surface.

(1) Define physical coefficients and boundary conditions for solving heat and mass transport equations. These includes

(a) Liquid thermal conductivity (κ_l) to solve equations (2) and (3)

(b) Solid thermal conductivity (κ_s) to solve equation (3)

(c) Latent heat of vaporization (L) to solve equation (**??**)

(d) Ambient temperature T_a, which is required in equation (5).

(e) Vapor saturation concentration $c_{sat}(T_a)$ at ambient temperature T_a.

(f) Rate $\left(\frac{\partial c}{\partial Tsat}\right)$ of change of vapor saturation concentration c_{sat} with temperature $\partial Tsat$.

(g) Relative humidity (H).

(2) Initial radius of curvature for the droplet and the droplet height are used to develop geometry and mesh for droplet and vapor region. The figure 3 illustrates the meshing of the droplet.

(3) Perform the numerical algorithm as obtained below.

Algorithm 1: Numerical Algorithm

[1] Initialize droplet temperature field T_d^j, solid temperature field T_s^i and vapor concentration field c^i

[2] Use concentration solution (c_i) and solid surface temperature gradient (∇T_s^i) to solve equation (1,3,2) to obtain droplet temperature field, which is denoted as $T_{d,sol}$.

[3] Set $Tdi = Td,sol$.

[4] Solve the transport equation for vapor concentration (4,5), which is denoted as $csol$.

[5] Set $c^i = c_{sol}$.

[6] Use concentration solution (c_i) and solid surface temperature gradient (∇T_s^i) to solve equation (1,3,2), to obtain $T_{d,sol}$.

[7] Estimate $Error_{dv} = max(\|T_{d,sol} - T_d^j\|)$

[8] **while** ($Error_{dv} > Error_{Tol}$) **do** [9] | Repeat steps (2,3,4,5,6,7).

[10] **end**

[11] Solve the transport equation for solid heat transport equation (8,5), which is denoted as $T_{s,sol}$.

[12] Set $T_s^i = T_{s,sol}$.

[13] Use concentration solution (c^i) and solid surface temperature gradient (∇T_s^i) to solve equation (1,3,2) to obtain $T_{d,sol}$.

[14] Estimate $Error_{sd} = max(\|T_{d,sol} - T_d^j\|)$

[15] **while** ($Error_{sd} > Error_{Tol}$) **do** [16] | Repeat steps (11,12,13,14).

[17] **end**

[18] Estimate $Error_{dv} = max(\|T_{d,sol} - T_d^j\|)$

[19] **while** ($Error_{dv} > Error_{Tol}$) **do**

[20] | Repeatsteps(2 – 18).

[21] **end**

4. EXPERIMENTAL RESULTS

The figure 4 obtains the experimental results for the variation of droplet evaporation time with varying base temperature and humidity. Further, the figure obtains the experimental results with two different solid substrate. These are aluminium and mild steel. Both the substrates aluminium and mild steel ,the rate of evaporation increases with the increase of base temperature and consequently the total time of evaporation decreases for the high conductive substrate with increase in the base temperature. The effect of relative humidity was also found to play an important role in decreasing the evaporation rate with increase in value of RH.This is because of the more vapour environment surrounding the water droplet with the increase in the RH.The high conductive substrate also enhances more evaporation at low RH value.

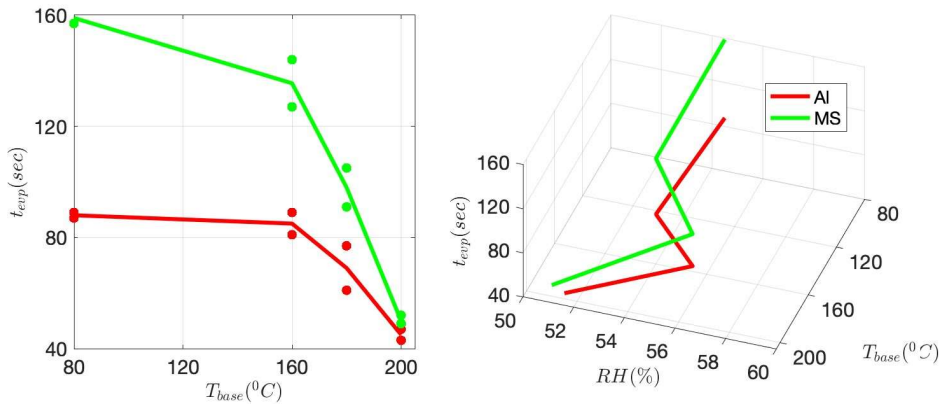

Figure 4. Figure depicts the experimental results for droplet evaporation rate plotted against base temperature and relative humidity.

5. NUMERICAL RESULTS

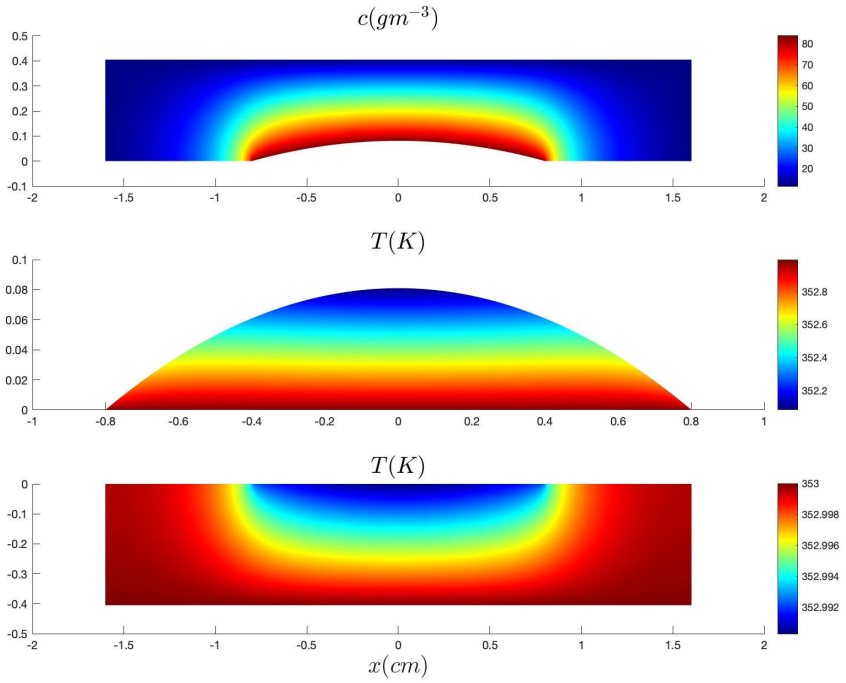

Figure 5. Figure depicts the numerical results for droplet evaporation temperature, vapor concentration in the droplet surrounding for water and base plate temperature distribution when Aluminum is used as base plate for water droplet.

The figure 5 obtains the numerical results for the variation of droplet evaporation

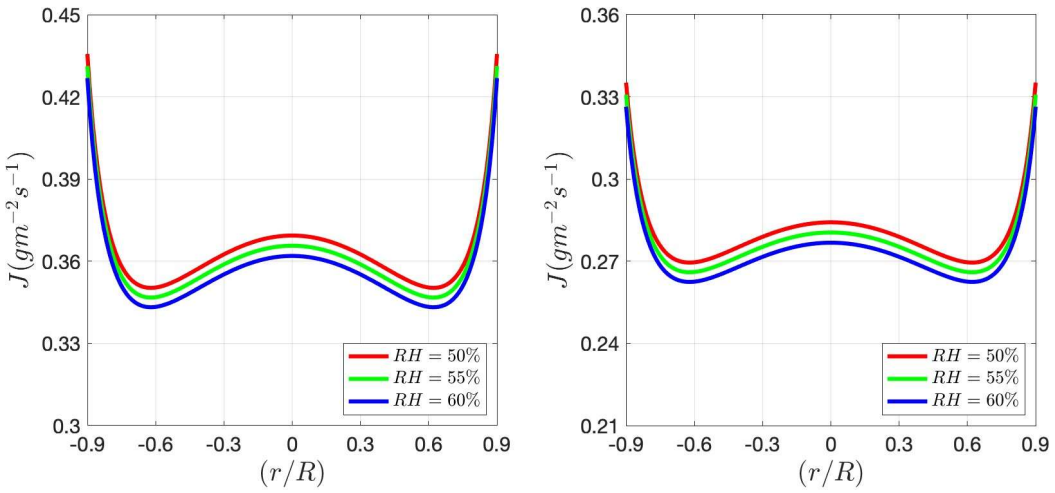

Figure 6. Figure depicts the numerical results for droplet evaporation flux for water droplet placed over Aluminum base plate for three different humidity and two base plate temperature (left plot is for 373K and the right plot is for 353K).

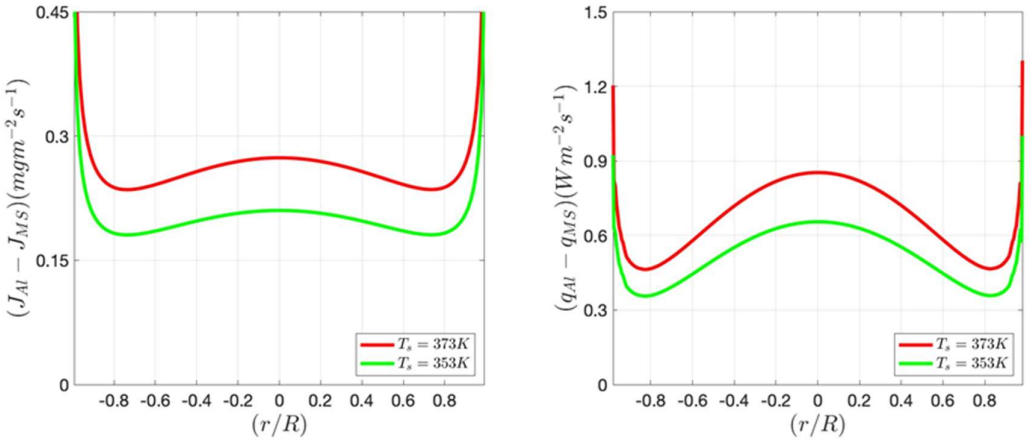

Figure 7. Figure compares the numerical results for the difference of droplet evaporation flux for water droplet and heat flux on the base plate between Aluminum and mild steel at two different temperature.

concentration profile over the droplet surface. The concentration is maximum just above the outer surface of the droplet and the evaporation concentration decreases as we move far away from the droplet top surface in upward direction and along radially outward direction. The numerical result also shows the temperature variation within the droplet. It is found that the temperature is maximum at the base of the droplet where it is in contact with the substrate and then the temperature decreases with the distance from the substrate as we move towards the top surface in perpendicular direction to the substrate. Similarly the variation of temperature along the substrate depth is also depicted by the numerical result. It is observed that with respect to the depth of the substrate ,the temperature increases until is achieves maximum value of the base temperature . The base temperature drops to the minimum value at the contact interface of the droplet. This is because of the local value of the heat transfer coefficient and the initiation of the convection phenomena at the interface of the substrate and the droplet.

Figure 6 depicts the numerical results for droplet evaporation flux for water droplet placed over Aluminum base plate for three different humidity at two base plate temperatures. The evaporation flux is maximum at the droplet contact with the surface. It is then reducing and achieves a minimum in an intermediate radius between droplet center and droplet edge. Thereafter, it increases again up to the droplet center. Droplet center also obtains a local maximum for evaporation flux. This explains as why during evaporation the contact radius decreases first and then there is decrease in height of the droplet. The profile of evaporation flux remains similar with changing relative humidity. However, there is a small decrease in the absolute values of evaporation flux with increasing RH. The evaporation flux is less resisted by the low humid surrounding and vice versa. By comparing the evaporation flux in the left

and right plots of figure 3, it can be concluded that evaporation flux increases with increase in base temperature. There is about 25% increase in evaporation flux with the change of temperature by 80 degree Celsius for Aluminum base plate.

In order to estimate the role of substrate's surface conducting properties in droplet evaporation, the numerical simulation is performed and compared for two different base plate types in the figure 7. The substrates compared are for Aluminum and Mild steel. The reported results depict the difference in mass flux on the droplet surface for Aluminum (Al) and Mild Steel (MS). The results are plotted in *milligram/m*^{2}*/s*. Further, the difference in heat flux on the substrate surface for AL and MS are also obtained in the right plot of figure 5. As expected, due to higher heat conductivity, Al has higher heat flux compared to MS. This leads to higher mass flux on the droplet surface for Al compared to MS. Difference of both heat and mass flux are highest at the droplet edge compared to the droplet center. Both the flux profile also achieves a minimum at an intermediate region between two droplet edge and center. Both heat and mass flux difference remain approximately same at the edges of droplet with variation in temperature. However, substantial changes in the heat and mass flux are observed in the central region of droplet. Therefore, it can be concluded that with increase in temperature, the effect of higher surface conductivity is more prominent around droplet central region compared to droplet edges.

6. CONCLUSION

In this paper, a controlled experiment is performed to quantitatively estimate the role of substrate surface conductivity on the droplet evaporation. The choice of Aluminum and Mild Steel as substrate surface allows to analyze the droplet properties for a variation of about eight times in substrate surface conductivity. Further, the effect of local humidity and base plate temperature is reported in the experiment. In addition to that, numerical simulation algorithm is developed to obtain the solution for vapor concentration, droplet temperature and base plate temperature. This further provides the solutions for heat and mass flux on substrate and droplet surface respectively. The coupled system of equations for heat and mass transport are solved in segregated manner and the solutions are obtained using iterative convergence criterion. The obtained results reported an enhanced heat and mass flux with increase in substrate heat conductivity. Further, enhanced humidity reduces the mass flux and increase in base plate temperature increase the mass flux. The difference between heat and mass flux of higher and lower conductive substrate increases with increase in base plate temperature.

REFERENCES

[1] R. G. Picknett, R. Bexon, J. Colloid Interface Sci. 61 (1977) 336.

[2] Y. O. Popov, Emerging structural understanding of amyloid fibrils by solid-state nmr, Phys. Rev. E. 71 (036313) (2005).

[3] C. Poulard, G. Gu´ena, A. M. Cazabat, Diffusion-driven evaporation of sessile drops, J. Phys. Condens. Matter 17 (2005) 4213–4227.

[4] N. N. Lebedev, Special Functions and Their Applications, Prentice Hall, 1965.

[5] C. Bourges-Monnier, M. E. R. Shanahan, Influence of evaporation on contact angle, Langmuir 11 (1995) 2820–2829.

[6] R. D. Deegan, O. Bakajin, T. F. Dupont, G. Huber, S. R. Nagel, T. A. Witten, Capillary flow as the cause of ring stains from dried liquid drops, Nature 389 (1997) 827–829.

[7] R. D. Deegan, O. Bakajin, T. F. Dupont, G. Huber, S. R. Nagel, T. A. Witten, Contact line deposits in an evaporating drop., Phys. Rev. Lett. 62 (2000) 756–765.

[8] H. Hu, R. G. Larson, Evaporation of a sessile droplet on a substrate, J. Phys. Chem. B 106 (2002) 1334–1344.

[9] H. Hu, R. G. Larson, Analysis of the effects of marangoni stresses on the microflow in an evaporating sessile droplet, Langmuir 21 (2005) 3972–3980.

[10] H. Hu, R. G. Larson, Analysis of the microfluid flow in an evaporating sessile droplet, Langmuir 21 (2005) 3963–3971.

[11] W. D. Ristenpart, P. G. Kim, C. Domingues, J. Wan, H. A. Stone, Influence of substrate conductivity on circulation reversal in evaporating drops, Phys. Rev. Lett. 99 (2007) 234502–1– 234502–4.

[12] F. Wang, J. Yao, S. Yang, R. Liu, J. Jin, A new stationary droplet evaporation model and its validation, Chinese Journal of Aeronautics 30 (2017) 1407–1416.

[13] S. Tonini, G. E. Cossali, E. A. Shchepakina, V. A. Sobolev, S. S. Sazhin, A model of droplet evaporation: New mathematical developments, Physics of Fluids 34 (2022) 073312.

[14] V. Charitatos, T. Pham, S. Kumar, Droplet evaporation on inclined substrates, Phys. Rev. Fluids 6 (2021) 084001.

[15] L. T. Raju, C. D. and Y. Li and A. Marin and M. N. van der Linden and X. Zhang and D. Lohse, Evaporation of a sessile colloidal water glycerol droplet: Marangoni ring formation, Langmuir 38 (2022) 12082–12094.

[16] G. J. Dunn, S. K. Wilson, B. R. Duffy, S. David, K. Sefiane, The strong influence of substrate conductivity on droplet evaporation, Journal of Fluid Mech. 623 (2009) 329– 351.